

An Analytical Model for the Impulse Response of Laminar Premixed Flames to Equivalence Ratio Perturbations

A. Albayrak, R.S. Blumenthal, A. Ulhaq, W. Polifke*

*Professur für Thermofluidodynamik, Technische Universität München,
Boltzmannstr. 15, D-85748 Garching, Germany*

Corresponding author

Wolfgang Polifke

Total length of paper

5796 words (method 2)

Mailing address

Professur für Thermofluidodynamik
Technische Universität München
Boltzmannstr. 15
D-85748 Garching, Germany

Main text 4689 words**References** 266 words

Fig. 1 101 words

Fig. 2 110 words

Fax +49 (0)89 / 289 16218

Fig. 3 110 words

Email polifke@tfd.mw.tum.de

Fig. 4 132 words

Intended colloquium

Fig. 5 101 words

for review:

Fig. 6 78 words

15 (CCs and CCCs only)

Fig. 7 110 words

for presentation:

13 - Gas Turbine Combustion

Fig. 8 99 words

alternative:

4 - Laminar Flames

*Corresponding author

Email address: polifke@tfd.mw.tum.de (W. Polifke)

Abstract

The dynamic response of conical laminar premixed flames to fluctuations of equivalence ratio is analyzed in the time domain, making use of a level set method ("G-Equation"). Perturbations of equivalence ratio imposed at the flame base are convected towards the flame front, where they cause modulations of flame speed, heat of reaction and flame shape. The resulting fluctuations of heat release rate are represented in closed form in terms of respective impulse response functions. The time scales corresponding to these mechanisms are identified, their contributions to the overall flame impulse response are discussed. If the impulse response functions are Laplace transformed to the frequency domain, agreement with previous results for the flame frequency response is observed. An extension of the model that accounts for dispersion of equivalence ratio fluctuations due to molecular diffusion is proposed. The dispersive model reveals the sensitivity of the premixed flame dynamics to the distance between the flame and the fuel injector. The model results are compared against numerical simulation of a laminar premixed flame.

Keywords

Laminar premixed flame dynamics, Equivalence ratio perturbation, Impulse response, Flame frequency response, Dispersion

1. Introduction

Modern low-emission combustion processes often utilize premixed combustion with lean fuel-air mixtures. However, premixed combustion is prone to thermo-acoustic instabilities, where positive feedback between fluctuating heat release and acoustics drives self-excited oscillations. Large amplitude oscillations can cause damage to a combustor, thus it is necessary to understand the physics of lean premixed combustion dynamics and reveal key factors and interaction mechanisms responsible for instabilities.

Premixed flame dynamics is driven mainly by velocity and equivalence ratio perturbations. The corresponding interaction mechanisms have been studied extensively by means of analytical models, numerical simulations and experiments, as described by Lieuwen [1]. First analytical studies of the dynamic response of anchored premixed flames to velocity perturbation were carried out by Boyer and Quinard [2] and Fleifil *et al.* [3]. Schuller *et al.* [4] presented a comprehensive treatment for various flame shapes, and compared analytical results against numerical and experimental data. All these studies were based on a linearized version of the so-called *G-Equation*, i.e. a kinematic equation for a propagating flame front [5]. Using the same framework, the response of laminar premixed flames to equivalence ratio perturbations was studied by Dowling and Hubbard [6] and by Lieuwen and co-workers [7–9].

The conventional way of representing the flame response to both velocity and equivalence ratio perturbations relies on the *Flame Transfer Functions* (FTF) in the frequency domain. Such a frequency domain approach is very convenient for asymptotic stability analysis, but poses a challenge for the

26 physics-based interpretation of transient flow–flame interactions. A time do-
27 main approach, based on the *Impulse Response* (IR) function, appears more
28 suitable for this purpose, even though fundamentally FTF and IR contain the
29 same information. The IR of premixed flames to velocity perturbations was
30 determined by Blumenthal *et al.* [10] using the linearized G -Equation. The
31 time domain perspective allowed straightforward identification of character-
32 istic time scales and gave additional insight into the pertinent flow–flame
33 interactions. Moreover, complete correspondence with frequency domain re-
34 sults by Schuller *et al.* [4] could be established.

35 In the present work, the impulse response of a conical premix flame to
36 perturbations of equivalence ratio is derived analytically. Following Lieuwen
37 and co-workers [7–9], the dominant interaction mechanisms between fluctu-
38 ations of equivalence ratio and heat release rate are considered (see Fig. 1):
39 Firstly, perturbations in equivalence ratio modulate the heat of reaction and
40 the laminar flame speed, which affect the heat release rate of the flame in a
41 direct manner [11, 12]. Moreover, changes in laminar flame speed disturb the
42 kinematic balance between flow and flame, such that the flame shape and the
43 flame surface area are also perturbed. This is an indirect, but important ef-
44 fect, first discussed by Lawn and Polifke [11]. Other contributions, i.e. flame
45 stretch and curvature, gas expansion, flame confinement and anchoring, are
46 not considered in the present analysis.

47 Like earlier studies [2–4, 7–9], the present work uses the linearized G -
48 Equation, but in the time domain. More insight into the physics of flame
49 dynamics is expected to result from such a treatment. It will be confirmed
50 that the overall flame dynamics can be described by the superposition of the

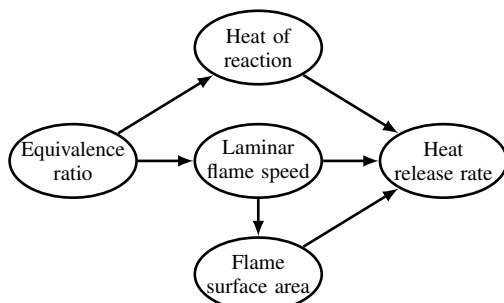


Figure 1: Major mechanisms contributing to heat release rate oscillations [7]

51 mechanisms depicted in Fig. 1. The respective contributions to the overall
 52 flame response are determined by individual IRs and relevant time scales are
 53 identified. Furthermore, an extension of the model is proposed, which consid-
 54 ers the effect of dispersion on the spatio-temporal distribution of equivalence
 55 ratio perturbations and on the flame dynamics.

56 The paper is structured as follows: A model for premixed flame dynamics
 57 based on the linearized G -Equation is described in the next section. Heat
 58 release rate fluctuations caused by perturbations of equivalence ratio are de-
 59 scribed in terms of impulse responses. For each of the contributions depicted
 60 in Fig. 1, the respective IR is derived and explained in Section 3. Eventu-
 61 ally the flame transfer functions of Shreekrishna *et al.* [8] are recovered. In
 62 Section 4, the dispersive model is introduced. Results of a validation study
 63 against numerical simulation is presented in Section 5.

64 2. Modeling Tools

65 2.1. Modeling of Heat Release Rate Fluctuations

66 Flame dynamics can be investigated with the relation $q(t) = \int_f \rho \Delta H s_L dA$
67 for the unsteady heat release rate of a premixed flame in linearized form

$$\frac{q'(t)}{\bar{q}} = \int_f \frac{\Delta H'}{\Delta \bar{H}} \frac{dA}{\bar{A}} + \int_f \frac{s'_L}{\bar{s}_L} \frac{dA}{\bar{A}} + \frac{A'(t)}{\bar{A}}, \quad (1)$$

68 where $(\bar{\quad})$ and $(\quad)'$ stand for the steady and fluctuating quantities, respectively.
69 ΔH is the heat of reaction, s_L is the laminar flame speed and A is the
70 flame surface area. The fluctuating quantities depend on the local values of
71 equivalence ratio ϕ . The unburnt gas density ρ is assumed to be constant.
72 The major contributions to heat release rate fluctuations discussed above
73 (see Fig. 1) appear explicitly on the r.h.s. of the equation.

74 2.2. *G*-Equation Approach for Flame Shape

75 The flame surface motion is modeled with the *G*-Equation, i.e. a level set
76 approach that reads

$$\frac{\partial G}{\partial t} + \vec{v} \cdot \vec{\nabla} G = s_L |\vec{\nabla} G|. \quad (2)$$

77 Here \vec{v} is the flow velocity and G is the level set function with the flame
78 position at $G = 0$. The linearized *G*-Equation can be solved analytically for
79 uniform mean velocity $\vec{v} = (0, \bar{v})$, see Fig. 2. The assumption of linearity
80 limits any perturbations to small amplitudes in order to have an amplitude
81 independent flame response. The flame aligned coordinate system " (X, Y) "
82 is employed instead of the laboratory coordinate system " (x, y) ", see Fig. 2.
83 The flame surface motion is assumed to be strictly normal to the flame,

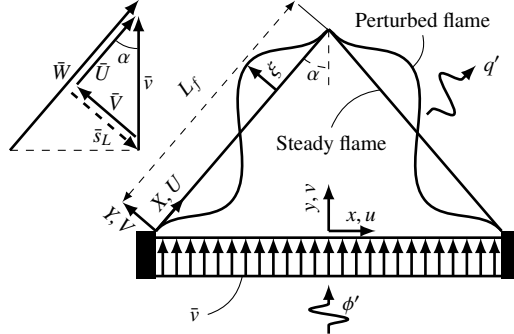


Figure 2: Flame configuration, important velocities and laboratory (x, y) and flame aligned (X, Y) coordinate systems

84 mathematically $G(X, Y, t) = Y - \xi(X, t)$. Substituting the perturbation in
 85 flame surface position $\xi(X, t)$ in the linearized G -Equation leads to

$$\frac{\partial \xi}{\partial t} + \bar{U} \frac{\partial \xi}{\partial X} = V' - s'_L. \quad (3)$$

86 The velocities U , V and s_L are illustrated in Fig. 2. The flame is assumed
 87 to be attached to the wall corners, i.e., $\xi(0, t) = 0$ is used as boundary
 88 condition. The analytical solution of Eq. (3) will be employed to determine
 89 the contribution of flame surface area fluctuations to the heat release rate in
 90 Section 3.3.

91 2.3. Impulse Response (IR) for Identification

92 A general way to quantify linear fluctuations in heat release rate q' caused
 93 by equivalence ratio perturbations ϕ' is the *impulse response* $h(\tau)$, which is
 94 defined implicitly via

$$\frac{q'(t)}{\bar{q}} = \frac{1}{\bar{\phi}} \int_0^\infty h(\tau) \phi'(y=0, t-\tau) d\tau. \quad (4)$$

95 Here the source of ϕ' is located at flame base $y = 0$ without loss of generality.
 96 If an impulse perturbation $\phi'(y=0, t) = \bar{\phi} \varepsilon \delta(t)$ is imposed, where δ is the

97 Dirac delta function and ε the relative strength of the perturbation, then
 98 correspondingly $q'(t)/\varepsilon\bar{q} = h(t)$, which is why $h(\tau)$ is called the *impulse*
 99 *response*. The effects that contribute to flame response – see Fig. 1 and
 100 Eq. (1) – can be investigated separately,

$$h(t) = h_{\Delta H}(t) + h_{s_L}(t) + h_A(t). \quad (5)$$

101 The FTF $F(\omega)$ is obtained from the IR by Laplace transformation, $F(s) =$
 102 $\int_0^\infty e^{-st}h(t) dt$ with $s = -i\omega$.

103 2.4. Transport of Equivalence Ratio Perturbations

104 The convective transport of equivalence ratio perturbations may be mod-
 105 eled with the 1-D advection equation as

$$\frac{\partial \phi'}{\partial t} + \bar{v} \frac{\partial \phi'}{\partial y} = 0. \quad (6)$$

106 The analytical solution for an impulse perturbation imposed at flame base
 107 $y = 0$ reads

$$\phi'(x, y, t) = \bar{\phi}\varepsilon\delta\left(t - \frac{y}{\bar{v}}\right) = \bar{\phi}\varepsilon\delta\left(t - \frac{X}{\bar{W}}\right). \quad (7)$$

108 Physically interpreted, a sudden change in equivalence ratio at the flame
 109 base convects in y -direction towards the flame tip with the flow velocity \bar{v} .
 110 Eq. (7) also shows how this effect may be represented in the flame-aligned
 111 coordinate system.

112 3. Contributions to the Flame Impulse Response

113 3.1. Fluctuations of Heat of Reaction

114 The first term on the right hand side of Eq. (1) stands for the contribution
 115 of heat of reaction fluctuations to the heat release rate. The fluctuation

116 in heat of reaction $\Delta H'$ caused by the equivalence ratio perturbations ϕ'
 117 is approximated by a relation $\Delta H = f(\phi)$ from empirical data (valid for
 118 CH_4 [7]). First order Taylor series expansion is employed for fluctuating
 119 quantities, $\Delta H' = d\Delta H/d\phi|_{\phi=\bar{\phi}} \phi'$.

120 By integrating $\Delta H'$ over the flame surface, the IR contribution is calcu-
 121 lated as

$$h_{\Delta H}(t) = \frac{1}{\varepsilon} \int_f \frac{\Delta H'}{\Delta \bar{H}} \frac{dA}{\bar{A}} = \frac{1}{\varepsilon} \left. \frac{d\Delta H}{d\phi} \right|_{\phi=\bar{\phi}} \frac{1}{\Delta \bar{H} \bar{A}} \int_f \phi' dA, \quad (8)$$

122 where $\bar{A} = \pi L_f^2 \sin \alpha$ is the steady flame surface area and $dA = 2\pi(L_f -$
 123 $X) \sin \alpha dX$ is the steady infinitesimal flame surface area for a conical flame.
 124 By substituting $\phi' = \bar{\phi} \varepsilon \delta(t - X/\bar{W})$ as defined in Section 2.4, the IR is
 125 obtained in closed form

$$h_{\Delta H}(t) = \frac{2S_{\Delta H}}{\tau_c^2} \{R(t - \tau_c) - R(t) + \tau_c H(t)\}. \quad (9)$$

126 where $H(t)$ is the Heaviside function and $R(t)$ is the Ramp function. $S_{\Delta H} =$
 127 $(\bar{\phi}/\Delta \bar{H}) d\Delta H/d\phi|_{\phi=\bar{\phi}}$ is the sensitivity of the heat of reaction to the equiv-
 128 alence ratio. $\tau_c = L_f/\bar{W}$ is a convective time scale, which is defined as the
 129 time span for the perturbation to travel from the base of the flame to its tip.
 130 The IR according to Eq. (9) is plotted in Fig. 3 with the solid line.

131 Laplace Transform as defined in Section 2.3 recovers exactly the analytical
 132 expression for the flame transfer function obtained by Shreekrishna *et al.* [8,
 133 Eq. (25)].

134 For the lean premixed flame, a positive impulse perturbation in the equiv-
 135 alence ratio increases the heat of reaction on the flame surface element located
 136 at the instantaneous position of the perturbation. The increase in heat of

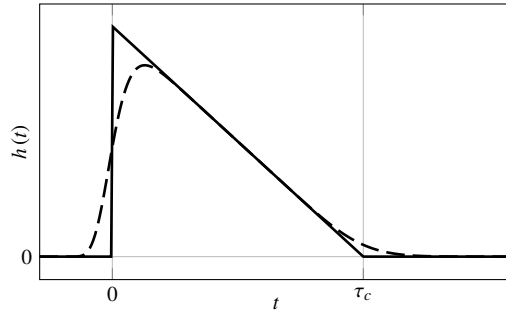


Figure 3: Contribution of fluctuations in heat of reaction or laminar flame speed to the IR. Models without (—) and with dispersion (---)

137 reaction also increases the heat release rate (see Eq. (1)). In Fig. 4 a flame
 138 perturbed by a δ -pulse as defined in Eq. (7) is shown. The upper gray line
 139 ("Perturbation, \bar{W} ") indicates the flame surface element, whose heat of reac-
 140 tion is changed. The incoming perturbation initially acts on the flame at the
 141 base, which has the largest radius. As the perturbation is convected towards
 142 the flame tip, the resulting perturbation in heat release rate decreases, be-
 143 cause the radius of the flame decreases. This fact explains the trend shown
 144 in Fig. 3, that the IR contribution is highest at the beginning and decreases
 145 until the convective time scale τ_c , when the perturbation reaches the flame
 146 tip, which has zero radius.

147 For rich mixtures, additional fuel barely changes the heat of reaction,
 148 which implies that the sensitivity $S_{\Delta H}$ and thus also the corresponding IR
 149 are very small.

150 3.2. Fluctuations of Laminar Flame Speed

151 The second term on the right hand side of Eq. (1) stands for the contri-
 152 bution of laminar flame speed fluctuations to the heat release rate. The same
 153 approach as described in Section 3.1 is employed also for laminar flame speed

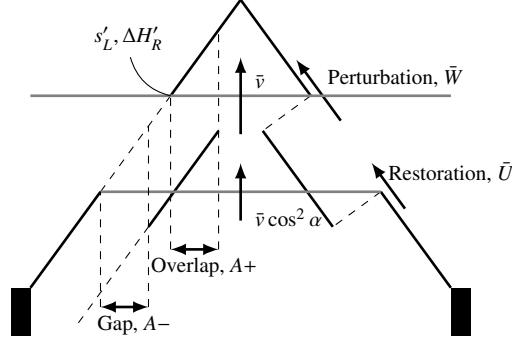


Figure 4: Intermediate flame shape with relevant velocities for convection of perturbation and restoration process. Visualization of area gap and overlap due to the change in laminar flame speed

154 contribution. The only difference is that $S_{\Delta H}$ is replaced with the sensitivity
 155 of laminar flame speed to the equivalence ratio, $S_{s_L} = (\bar{\phi}/\bar{s}_L) ds_L/d\phi|_{\phi=\bar{\phi}}$.
 156 The shape of the corresponding IR is shown in Fig. 3 and can be explained
 157 with similar arguments as in Section 3.1. Again, Laplace Transform recovers
 158 exactly the FTF of Shreekrishna *et al.* [8, Eq. (24)].

159 For lean premixed flames the sensitivity S_{s_L} is positive and therefore the
 160 IR is positive. For rich mixtures, additional fuel leads to a decrease in the
 161 laminar flame speed and the IR is reversed.

162 3.3. Fluctuations of Flame Surface Area

163 The third term on the right hand side of Eq. (1) stands for the contri-
 164 bution of flame surface area fluctuations to the IR of the heat release rate.
 165 This mechanism was already discussed by Blumenthal *et al.* [10], albeit only
 166 for the perturbations in velocity. Relevant time scales of restoration τ_r and
 167 convection τ_c were revealed, their impact on flame dynamics was discussed.
 168 In the present study, a similar approach is developed for the effects of equiva-

169 lence ratio perturbations on flame shape and heat release rate. The similarity
 170 comes from the fact that the perturbed flame position ξ depends on V' and
 171 s'_L , as described in the right hand side of Eq. (3). The similarity is attributed
 172 to Eq. (3), where V' and s'_L act as source terms for the perturbed flame po-
 173 sition ξ .

174 The first step is to compute ξ . The Eq. (3) for $\xi(X, t)$ can be formulated
 175 as an integral equation

$$\xi(X, t) = -\frac{1}{\bar{U}} \int_0^X s'_L \left(X', t - \frac{X - X'}{\bar{U}} \right) dX', \quad (10)$$

176 where laminar flame speed fluctuations caused by ϕ' are considered solely
 177 ($V' = 0$). The IR contribution is calculated as

$$h_A(t) = \frac{1}{\varepsilon} \frac{A'(t)}{\bar{A}} = \frac{2}{\varepsilon L_f^2 \tan \alpha} \int_0^{L_f} \xi(X, t) dX. \quad (11)$$

178 In order to calculate the closed form IR, $\phi' = \bar{\phi} \varepsilon \delta(t - X/\bar{W})$ is substituted
 179 in Eq. (10) and ξ is expressed as

$$\xi(X, t) = - \left. \frac{ds_L}{d\phi} \right|_{\phi=\bar{\phi}} \frac{\bar{\phi} \varepsilon \tau_r}{\tau_r - \tau_c} \left[H \left(t - \frac{X}{\bar{W}} \right) - H \left(t - \frac{X}{\bar{U}} \right) \right], \quad (12)$$

180 where $\tau_r = L_f/\bar{U}$ is the restorative time scale, which is defined as the time
 181 span for the hypothetical restoration line to travel from the base of the flame
 182 to its tip. ξ is illustrated with an intermediate flame shape perturbed with
 183 an impulse in Fig. 4.

184 The upper gray line ("Perturbation, \bar{W} ") indicates the convection of im-
 185 pulsive perturbation and $\bar{W} = \bar{v}/\cos(\alpha)$ is the projection on X -direction.
 186 Since the mixture is assumed lean and the equivalence ratio perturbation is
 187 positive, the laminar flame speed perturbation is also positive. An increase in

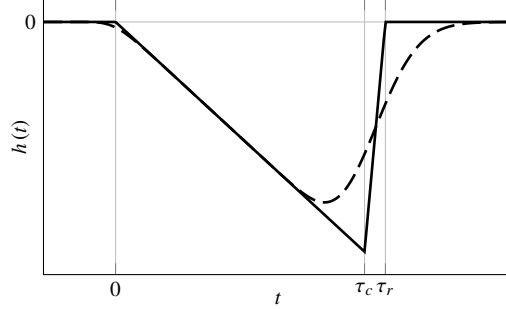


Figure 5: Contribution of fluctuations of flame surface area to IR. Model without (—) and with dispersion (— —)

188 laminar flame speed overcomes the flow velocity normal to the flame surface
 189 and the flame propagates towards the base.

190 Starting from the anchoring point, where $\xi(0, t) = 0$, the restoration
 191 mechanism [10] re-establishes the original, unperturbed flame shape after the
 192 perturbation of equivalence ratio has passed. The lower gray line ("Restora-
 193 tion, \bar{U} ") in Fig. 4 indicates up to which position the restoration process has
 194 progressed. This line travels with the speed $U = \bar{v} \cos(\alpha)$ in X -direction.
 195 The restoration line is upstream of the perturbation line, because of slower
 196 propagation speed.

197 By substituting ξ described in Eq. (12) into Eq. (11), the closed form IR
 198 is obtained

$$h_A(t) = - \frac{2S_{sL}}{\tau_c(\tau_r - \tau_c)} \times \left[\frac{\tau_c}{\tau_r} \{R(t - \tau_r) - R(t)\} - \{R(t - \tau_c) - R(t)\} \right] \quad (13)$$

199 which is plotted in Fig. 5 with the solid line. Again the FTF given by
 200 Shreekrishna *et al.* [8, Eq. (26)] is exactly recovered by Laplace Transform.

201 The shape of the IR may be explained as follows: The perturbation ϕ'

202 causes flame propagation towards the base and creates additional flame sur-
203 face area indicated as "Overlap, A^+ " in Fig. 4. At the same time, the restora-
204 tion mechanism brings the flame to its old position and causes a deficit in
205 flame surface area indicated as "Gap, A^- " in Fig. 4. Since the restoration
206 process is slower, it acts at a position where the flame radius is larger than
207 the one for the perturbation, thus the perturbed area is less than the steady
208 area (negative IR in Fig. 5). As long as both processes act on the flame
209 together, the deficit of flame surface area continuously increases. At late
210 times $t > \tau_c$, when the perturbation has passed the flame, only the restora-
211 tive mechanism acts to recover the original flame shape. The flame surface
212 area deficit vanishes once the restoration line reaches the flame tip, which
213 corresponds to the restorative time scale τ_r .

214 This section concludes with a comment on the study of Cho *et al.* [7], who
215 derived time domain representations of flame dynamics by inverse Laplace
216 transformation of frequency domain results. However, the IR was not recov-
217 ered, because a generic form of perturbations was considered instead of an
218 impulse perturbation. A full time domain analysis of the flame response to
219 a generic perturbation is not straightforward and was indeed not attempted
220 by Cho *et al.* [7]. Instead, their results are valid only in the low-frequency,
221 quasi-steady limit.

222 4. Extended Model with Dispersion

223 In typical technical premixed combustion systems, the fuel is injected
224 from a considerable distance upstream of the flame. This distance is im-
225 portant for the equivalence ratio perturbations because of dispersion due

226 to molecular diffusion for a laminar flame. Generalization to turbulent dis-
 227 persion is straightforward, but not discussed further here (refer to Polifke
 228 *et al.* [13], Lawn and Polifke [11], Schuermans *et al.* [12] and Bobusch *et*
 229 *al.* [14]). As the injection point moves further upstream, a wider Gaussian
 230 distribution instead of an impulse (Dirac function) arrives at the flame base
 231 and thus the impact on flame dynamics becomes weaker.

232 The model described in Section 2 and also previous models [7–9] employ
 233 an advection equation as described in Eq. (6). The impact of the species
 234 diffusion can be accounted by considering 1-D advection-diffusion equation
 235 with impulse perturbation at flame base $y = 0$, which reads

$$\frac{\partial \phi'}{\partial t} + v \frac{\partial \phi'}{\partial y} = D \frac{\partial^2 \phi'}{\partial y^2}, \quad (14)$$

236 where D is the averaged diffusion coefficient. The analytical solution reads

$$\phi'(x, y, t) = \bar{\phi} \varepsilon \sqrt{\frac{1}{\pi \tau_d t}} \exp \left[-\frac{1}{\tau_d t} \left(t - \frac{X}{\bar{W}} \right)^2 \right], \quad (15)$$

237 where $\tau_d = 4D/\bar{v}^2$ is the diffusive time scale, which describes the strength
 238 of the diffusion. The solution is expressed in the flame aligned coordinate
 239 system.

240 The formalism developed in Section 3 can also be applied to the extended
 241 model. For heat of reaction contribution, Eq. (8) is integrated with the dif-
 242 fusive perturbation Eq. (15) instead of the impulse Eq. (7) (same for laminar
 243 flame speed contribution). The resulting IR contribution reads

$$h_{\Delta H}(t) = \frac{S_{\Delta H}}{\tau_c^2} \left\{ \mathfrak{R}(t - \tau_c) - \mathfrak{R}(t) + \tau_c \operatorname{erf} \left(\frac{t}{\sqrt{\tau_d t}} \right) \right\}, \quad (16)$$

244 where $\mathfrak{R}(t, \tau)$ is the smoothed Ramp function defined as

$$\mathfrak{R}(t - \tau) = \sqrt{\frac{\tau_d t}{\pi}} \exp\left(-\frac{(t - \tau)^2}{\tau_d t}\right) + (t - \tau) \operatorname{erf}\left(\frac{t - \tau}{\sqrt{\tau_d t}}\right). \quad (17)$$

245 The contribution of laminar flame speed fluctuations is the same as Eq. (16),
246 but $S_{\Delta H}$ is replaced with S_{sL} .

247 For flame surface area contribution, the flame surface deviation ξ is de-
248 termined by integrating Eq. (10) again with the diffusive perturbation. The
249 contribution is then computed by integrating the flame surface deviation
250 Eq. (11) as

$$h_A(t) = -\frac{S_{sL}}{\tau_c (\tau_r - \tau_c)} \times \left[\frac{\tau_c}{\tau_r} \{ \mathfrak{R}(t - \tau_r) - \mathfrak{R}(t) \} - \{ \mathfrak{R}(t - \tau_c) - \mathfrak{R}(t) \} \right]. \quad (18)$$

251 The resulting IRs are plotted in Figs. 3 and 5 with dashed lines, for heat of
252 reaction (same for laminar flame speed) and flame surface area, respectively.

253 The model can be extended for the cases, where the perturbation is im-
254 posed upstream of the flame base, say $y = -y_0$. The additional time lag for
255 the perturbation to travel till the flame base $\tau_0 = y_0/\bar{v}$ can be accounted by
256 change of variable of $t = t^* - \tau_0$ in Eq. (15)–(18).

257 5. Validation against Numerical Simulation

258 A numerical simulation of a 2D axisymmetric conical flame is performed
259 to validate the analytical model. Length and radius of the upstream flow duct
260 are both 1 mm, the downstream radius of the computational domain is 6 mm
261 in order to prevent confinement effects. A uniform mesh is constructed with a

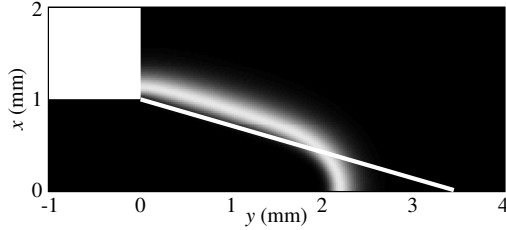


Figure 6: Flame shapes : G-equation model vs. numerical simulation with 2-step chemistry

262 cell size of 0.02 mm. Slip and adiabatic wall boundary conditions are imposed
 263 to correspond with the analytical framework. A lean mixture of CH_4 and air
 264 ($\bar{\phi} = 0.8$) is used, the inflow velocity is $\bar{v} = 1$ m/s (Reynolds number 130)
 265 at a temperature of 293 K. A 2-step reduced chemistry is employed [15] in
 266 rhoReactingFoam (OpenFOAM solver), which is modified to assume Prandtl
 267 number of 0.7. The averaged molecular diffusivity was set to $D = 0.22 \times$
 268 $10^{-4} \text{m}^2/\text{s}$, appropriate for CH_4 in air [16].

269 Fig. 6 compares the distribution of steady heat release rate from CFD
 270 against the analytical G -Equation flame. Close to the tip, curvature effects
 271 – which are not considered in G -equation used – result in a comparatively
 272 shorter flame length of the CFD model.

273 Broadband equivalence ratio perturbations with an amplitude of $\varepsilon =$
 274 $\phi'/\bar{\phi} = 0.05$ are imposed at the inlet. The corresponding IR is determined via
 275 system identification (for details see [17]) and compared against the analytical
 276 model in Fig. 7. The latter includes all three contributions discussed above,
 277 see Fig. 1.

278 Including dispersion in the analytical model gives a "smeared out" re-
 279 sponse, in qualitative agreement with CFD. More than that, Fig. 7 shows
 280 very good quantitative agreement between CFD and the dispersive model

281 for the early period $t < 2$ ms.

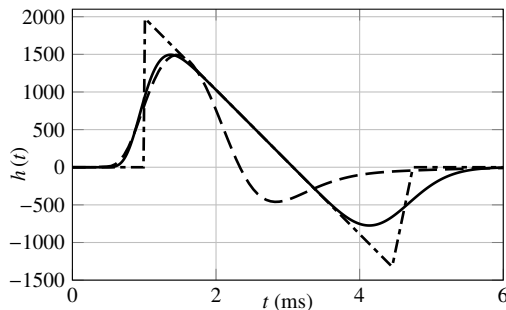


Figure 7: Impulse response functions of conical laminar premixed flame. Analytical model without dispersion (---), with dispersion (—) and CFD results (-.-)

282 At later times, the impulse response is negative before it decays to zero.
 283 This important feature, which is responsible for the excess gain of the FTF
 284 (see below) is reproduced qualitatively by both models based on the G-
 285 equation. Nevertheless, it is apparent that at later times $t > 2$ ms quan-
 286 titative agreement with CFD deteriorates. This is due to the over-predicted
 287 flame length of the G-equation model, resulting from the neglect of curvature
 288 effects. Note that the overall duration of the IR is related to the restorative
 289 time scale $\tau_r = L_f/\bar{U}$. Since the flame length L_f is over-predicted, the re-
 290 sulting IR is also more pronounced at late times.

291 Fig. 8 compares the gain of the FTFs determined with the analytical
 292 model and the CFD simulation, respectively. Important qualitative features
 293 are reproduced by both analytical model formulations: the overall low pass
 294 filter behavior is observed, initial overshoot in gain is present, the low fre-
 295 quency limit (see Polifke and Lawn [18]) is correctly captured as unity.

296 The dash-dotted line indicates the FTF from the analytical model without
 297 dispersion. The model shows oscillatory behavior in the high frequency range,

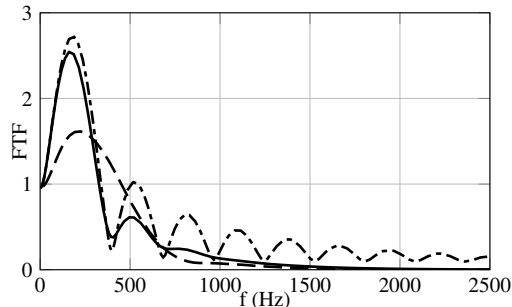


Figure 8: Gain of FTF. Analytical model without dispersion (---), with dispersion (—) and CFD results (- -)

298 which is eliminated by dispersion (shown with solid line).

299 Both analytical and numerical results exhibit excess gain $|FTF| > 1$ at
 300 frequencies around 200 Hz. Excess gain results from constructive superposi-
 301 tion of the positive and negative parts of the IR, as discussed by Huber and
 302 Polifke [19] and Blumenthal *et al.* [10]. The analysis in Section 3 has shown
 303 that the positive part of the IR results from fluctuations in heat of reaction
 304 and flame speed, while the negative part is due to the modulation of flame
 305 surface area. In the low frequency limit there is destructive superposition
 306 of these effects, which becomes constructive at intermediate frequencies, re-
 307 sulting in excess gain. Indeed, earlier models that did not take into account
 308 changes in flame surface area do not exhibit excess gain [13, 20].

309 The intermediate frequency f_{\max} where the gain attains its maximum can
 310 be roughly estimated as

$$f_{\max} \approx \frac{\pi}{2(t_{\max} - t_{\min})}, \quad (19)$$

311 where t_{\max} and t_{\min} are the times where the IR reaches maximal / minimal
 312 values. For the analytical model with dispersion, one estimates $f_{\max} \approx 200$
 313 Hz, which agrees with the gain of the FTF shown in Fig. 8. For the CFD

314 results, the negative part of the IR appears earlier and is less pronounced
315 (see Fig. 6), thus excess gain occurs at higher frequencies and with reduced
316 magnitude, as seen in Fig. 8.

317 6. Conclusion

318 The response of laminar premixed flame to equivalence ratio perturba-
319 tions was studied analytically by determining the IR for heat release rate.
320 In the framework of the G -Equation contributions of heat of reaction, lami-
321 nar flame speed and flame surface area were taken into consideration. Two
322 relevant time scales were identified, i.e. a convective time scale τ_c and a
323 restorative time scale τ_r . The transport of equivalence ratio perturbations
324 is related to τ_c , while the propagation of flame shape perturbations along
325 the flame is related to τ_r . The contributions of heat of reaction and laminar
326 flame speed are governed only by τ_c , since the convective perturbations of
327 equivalence ratio causes local changes at the flame surface. The contribution
328 of flame surface area is controlled by both τ_c and τ_r due to the restoration
329 mechanism. Complete agreement with flame transfer functions calculated by
330 Shreekrishna *et al.* [8] was established by Laplace transformation of IRs.

331 An extension to the model was proposed in order to account for the
332 dispersion due to molecular diffusion. The dispersive model adds one more
333 time scale τ_d regarding the strength of the dispersion. As the location of
334 the perturbation moves further away from the flame, its impact on the flame
335 dynamics becomes weaker [13].

336 Analytical models were compared against numerical simulation by exam-
337 ining the respective IRs and FTFs. Quantitative agreement was not achieved,

338 since the analytical G -Equation model used in this study neglects curvature
339 effects and thus over-predicts the flame length. Nevertheless, very satis-
340 factory qualitative agreement with respect to the shape of the IR and the
341 relevant time scales was observed. Overall, the model with dispersion showed
342 significantly better agreement than the model without dispersion.

343 The analysis in the paper shows that excess gain in the flame response to
344 equivalence ratio fluctuations results from constructive superposition of the
345 effects of fluctuations in heat of reaction and flame speed on the one hand,
346 and the effects of modulation of flame shape on the other.

347 **Acknowledgements**

348 The presented work is part of the Marie Curie Initial Training Network
349 *Thermo-acoustic and aero-acoustic nonlinearities in green combustors with*
350 *orifice structures* (TANGO). We gratefully acknowledge the financial sup-
351 port from the European Commission under call FP7-PEOPLE-ITN-2012.
352 Financial support for A. Ulhaq was provided by higher education commis-
353 sion (HEC) of Pakistan. Financial support for R. S. Blumenthal was provided
354 by Technische Universität München, Institute for Advanced Study, funded by
355 the German Excellence Initiative, and German Research Foundation DFG,
356 project PO 710/12-1.

357 **References**

- 358 [1] T. C. Lieuwen, *Unsteady Combustor Physics*, Cambridge University Press, 2012.
- 359 [2] L. Boyer, J. Quinard, *Combust. Flame* 82 (1990) 51–65.

- 360 [3] A. Fleifil, A. M. Annaswamy, Z. A. Ghoneim, A. F. Ghoniem, *Combust. Flame* 106
361 (1996) 487–510.
- 362 [4] T. Schuller, D. Durox, S. Candel, *Combust. Flame* 134 (2003) 21–34.
- 363 [5] A. R. Kerstein, W. T. Ashurst, F. A. Williams, *Phys. Rev. A* 37 (1988) 2728.
- 364 [6] A. Dowling, S. Hubbard, *Proceedings of the Institution of Mechanical Engineers, Part*
365 *A: Journal of Power and Energy* 214 (2000) 317–332.
- 366 [7] J. H. Cho, T. Lieuwen, *Combust. Flame* 140 (2005) 116–129.
- 367 [8] Shreekrishna, S. Hemchandra, T. Lieuwen, *Combust. Theor. Model.* 14 (2010) 681–
368 714.
- 369 [9] S. Hemchandra, in: *ASME Turbo Expo: Turbine Technical Conference and Exposi-*
370 *tion, GT2011-45590*, American Society of Mechanical Engineers, pp. 567–578.
- 371 [10] R. S. Blumenthal, P. Subramanian, R. Sujith, W. Polifke, *Combust. Flame* 160 (2013)
372 1215–1224.
- 373 [11] C. J. Lawn, W. Polifke, *Combust. Sci. Technol.* 176 (2004) 1359 – 1390.
- 374 [12] B. Schuermans, V. Bellucci, F. Guethe, F. Meili, P. Flohr, O. Paschereit, in: *Int’l*
375 *Gas Turbine and Aeroengine Congress & Exposition*, GT2004-53831.
- 376 [13] W. Polifke, J. Kopitz, A. Serbanovic, in: *7th AIAA/CEAS Aeroacoustics Conference*,
377 *AIAA 2001-2104*, Maastricht, The Netherlands.
- 378 [14] B. C. Bobusch, B. Ćosić, J. P. Moeck, C. Oliver Paschereit, in: *Journal of Engineering*
379 *for Gas Turbines and Power*, volume 136, San Antonio, Texas, USA, pp. 021506–
380 021506.
- 381 [15] J. Bibrzycki, T. Poinso, A. Zajdel, in: *Archivum combustionis*, volume 30, A.
382 *Teodorczyk*, Varsovie, Pologne, 2010, pp. 287–296.
- 383 [16] M. Cowie, H. Watts, *Can. J. Chem.* 49 (1971) 74–77.

- 384 [17] W. Polifke, *Annals of Nuclear Energy* 67C (2014) 109–128.
- 385 [18] W. Polifke, C. J. Lawn, *Combust. Flame* 151 (2007) 437–451.
- 386 [19] A. Huber, W. Polifke, *Int. J. Spray Combust. Dyn.* 1 (2009) 199–228.
- 387 [20] J. F. v Kampen, J. B. W. Kok, T. H. van der Meer, in: 12th Int. Congress on Sound
388 and Vibration (ICSV12), IIAV, Lisbon, Portugal, July 11-14 2005.

Preprint

An Analytical Model for the Impulse Response of Laminar Premixed Flames to Equivalence Ratio Perturbations

A. Albayrak, R.S. Blumenthal, A. Ulhaq, W. Polifke*

*Professur für Thermofluidodynamik, Technische Universität München,
Boltzmannstr. 15, D-85748 Garching, Germany*

Corresponding author

Wolfgang Polifke

Total length of paper

5796 words (method 2)

Mailing address

Professur für Thermofluidodynamik
Technische Universität München
Boltzmannstr. 15
D-85748 Garching, Germany

Main text 4689 words

References 266 words

Fig. 1 101 words

Fig. 2 110 words

Fax +49 (0)89 / 289 16218

Fig. 3 110 words

Email polifke@tfd.mw.tum.de

Fig. 4 132 words

Intended colloquium

Fig. 5 101 words

for review:

Fig. 6 78 words

15 (CCs and CCCs only)

Fig. 7 110 words

for presentation:

13 - Gas Turbine Combustion

Fig. 8 99 words

alternative:

4 - Laminar Flames

*Corresponding author

Email address: polifke@tfd.mw.tum.de (W. Polifke)

Abstract

The dynamic response of conical laminar premixed flames to fluctuations of equivalence ratio is analyzed in the time domain, making use of a level set method ("G-Equation"). Perturbations of equivalence ratio imposed at the flame base are convected along the flame front, where they cause modulations of flame speed, heat of reaction and flame shape. The resulting fluctuations of heat release rate are represented in closed form in terms of respective impulse response functions. The time scales corresponding to these mechanisms are identified, their contributions to the overall flame impulse response are discussed. If the impulse response functions are Laplace transformed to the frequency domain, agreement with previous results for the flame frequency response is observed. An extension of the model that accounts for dispersion of equivalence ratio fluctuations due to molecular diffusion is proposed. The dispersive model reveals the sensitivity of the premixed flame dynamics to the distance between the flame and the fuel injector. The model results are compared against numerical simulation of a laminar premixed flame.

Keywords

Laminar premixed flame dynamics, Equivalence ratio perturbation, Impulse response, Flame frequency response, Dispersion

1. Introduction

~~Due to the strict emission regulations combustion processes require leaner~~
~~Modern low-emission combustion processes often utilize premixed combustion~~
~~with lean~~ fuel-air mixtures. However, ~~lean-premixed~~ combustion is prone to
~~instabilities, which might cause damage to the combustor in the presence~~
~~of thermo-acoustic instabilities, where~~ positive feedback between fluctuating
heat release and acoustics ~~. Therefore, drives self-excited oscillations. Large~~
~~amplitude oscillations can cause damage to a combustor, thus~~ it is necessary
to understand the physics of lean premixed combustion dynamics and reveal
~~the key factors that are~~ key factors and interaction mechanisms responsible
for instabilities.

~~The flame dynamics are~~ Premixed flame dynamics is driven mainly by
velocity and equivalence ratio perturbations. The corresponding interaction
mechanisms have been ~~extensively studied~~ studied extensively by means of
analytical models, numerical simulations and experiments.

First analytical studies of the dynamic response of anchored premixed
flames to velocity perturbation were carried out by Boyer and Quinard [1]
and Fleifil *et al.* [2]. Schuller *et al.* [3] presented a comprehensive treatment
for various flame shapes, and compared analytical results against numerical
and experimental data. All these studies were based on a linearized version of
the so-called ~~G-equation~~ G-Equation, i.e. a kinematic equation for a ~~premixed~~
~~flame~~ [4]. ~~The propagating flame front~~ [4]. Using the same framework,
the response of laminar premixed flames to equivalence ratio perturbations
~~were studied subsequently~~ was studied by Dowling and Hubbard [5] and by

26 Lieuwen and co-workers~~[6–8]~~, ~~using the same framework~~ [8, 6, 7].

27 The conventional way of representing the flame response to both velocity
28 and equivalence ratio perturbations relies on the ~~Flame Transfer Functions~~
29 Flame Transfer Functions (FTF) in the frequency domain. Such a fre-
30 quency domain approach is very convenient for asymptotic stability analysis,
31 but ~~it~~ poses a challenge for ~~interpretation of the transient flow physics~~the
32 physics-based interpretation of transient flow–flame interactions. A time do-
33 main approach, based on the ~~Impulse Response~~ Impulse Response (IR) func-
34 tion, appears more suitable for this purpose, even though fundamentally FTF
35 and IR contain the same information. The IR of premixed flames to velocity
36 perturbations was determined by Blumenthal *et al.* [9] using the linearized
37 ~~G-equation. Complete correspondence with the Equation. The time domain~~
38 perspective allowed straightforward identification of characteristic time scales
39 and gave additional insight into the pertinent flow–flame interactions. Moreover,
40 complete correspondence with frequency domain results by Schuller *et al.* [3]
41 could be established. ~~More than that, the time domain approach gave~~
42 ~~additional insight into the physics of flow–flame interactions, with straightforward~~
43 ~~identification of characteristic time scales and their respective effects on the~~
44 ~~flame dynamics.~~

45 In the present work, the impulse response of a conical premix flame to
46 perturbations of equivalence ratio is derived analytically. Following Lieuwen
47 and co-workers~~[6–8]~~ [8, 6, 7], the dominant interaction mechanisms between
48 fluctuations of equivalence ratio and heat release rate are considered (see
49 Fig. 1): Firstly, perturbations in equivalence ratio modulate the heat of re-
50 action and the laminar flame speed, which affect the heat release rate of the

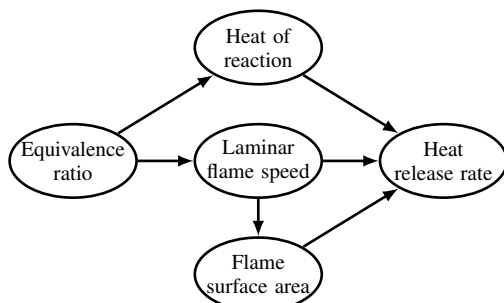


Figure 1: Major mechanisms contributing to heat release rate oscillations [8]

51 flame in a direct manner [10, 11]. Moreover, changes in laminar flame speed
 52 disturb the kinematic balance between flow and flame, such that the flame
 53 shape and the flame surface area are also perturbed. This is an indirect, but
 54 important effect, first discussed by Lawn and Polifke [10]. Other contribu-
 55 tions, i.e. flame stretch and curvature, gas expansion, flame confinement and
 56 anchoring, are not considered in the present analysis

57 Like earlier studies ~~[1-3, 6-8]~~ [1-3, 8, 6, 7], the present work uses the
 58 linearized ~~G -equation~~ Equation, but in the time domain. More insight into
 59 the physics of flame dynamics is expected to result from such a treatment.
 60 It will be confirmed that the overall flame dynamics can be described by the
 61 superposition of the mechanisms depicted in Fig. 1. The respective ~~impact~~
 62 ~~of each contribution on flame dynamics~~ contributions to the overall flame
 63 response is determined by individual IRs and relevant time scales are iden-
 64 tified. Furthermore, an extension of the model is proposed, which considers
 65 the effect of dispersion on the spatio-temporal distribution of equivalence
 66 ratio perturbations ~~along the flame~~ and on the flame dynamics.

67 The paper is structured as follows: ~~The model for heat release rate~~
 68 ~~fluctuations with~~ A model for premixed flame dynamics based on the lin-

earized ~~G-equation~~ Equation is described in the ~~following~~ Section. ~~The~~
~~impulse response (IR) approach is employed for identification of heat~~ next
~~section.~~ Heat release rate fluctuations caused by perturbations of equivalence
~~ratio are described in terms of impulse responses.~~ For each ~~contribution of~~
~~the contributions depicted in Fig. 1),~~ the respective ~~IRs are~~ IR is derived and
explained in Section 3. Eventually the flame transfer functions ~~derived by~~
~~of~~ Shreekrishna *et al.* [6] are recovered. In Section 4, the dispersive model
is introduced. Results of a validation study against numerical simulation is
presented in Section 5.

2. Modeling Tools

2.1. Modeling of Heat Release Rate Fluctuations

Flame dynamics can be investigated ~~using with the relation~~ $q(t) = \int_f \rho \Delta H s_L dA$
~~for the unsteady heat release rate equation for of~~ a premixed flame ~~$q(t) = \int_f \rho \Delta H s_L dA$~~
~~in-linearised in~~ linearized form

$$\frac{q'(t)}{\bar{q}} = \int_f \frac{\Delta H'}{\Delta \bar{H}} \frac{dA}{\bar{A}} + \int_f \frac{s'_L}{\bar{s}_L} \frac{dA}{\bar{A}} + \frac{A'(t)}{\bar{A}}, \quad (1)$$

where $(\bar{\quad})$ and $(\quad)'$ stand for the steady and fluctuating quantities, respectively.
 ΔH is the heat of reaction, s_L is the laminar flame speed and A is the flame
surface area. The fluctuating quantities depend on ~~local value~~ the local values
of equivalence ratio ϕ . The unburnt gas density ρ is assumed to be constant.
The major contributions ~~causing to~~ heat release rate fluctuations dis-
cussed above (see Fig. 1) appear explicitly on the ~~right hand side~~ r.h.s. of
the equation.

103 ~~where $\xi(X, t)$ is~~ the perturbation in flame surface position ~~– $\xi(X, t)$ in the~~
 104 ~~linearized G-Equation leads to~~

$$\frac{\partial \xi}{\partial t} + \bar{U} \frac{\partial \xi}{\partial X} = V' - s'_L. \quad (3)$$

105 The velocities U , V and s_L are illustrated in Fig. 2. The flame is assumed to
 106 be attached to the wall corners, i.e., $\xi(0, t) = 0$ is used as boundary condition.
 107 The analytical solution of Eq. (3) is employed to determine the contribution
 108 of flame surface area fluctuations to the heat release rate in Section 3.3.

109 2.3. Impulse Response (IR) for Identification

110 A general way to quantify linear fluctuations in heat release rate ~~\dot{q}'~~
 111 caused by equivalence ratio perturbations ϕ' is the *impulse response* $h(\tau)$
 112 which is defined implicitly via

$$\frac{q'(t)}{\bar{q}} = \frac{1}{\bar{\phi}} \int_0^\infty h(\tau) \phi'(y=0, t-\tau) d\tau. \quad (4)$$

113 Here the source of ϕ' is located at flame base $y = 0$ without loss of generality.
 114 If an impulse perturbation $\phi'(y=0, t) = \bar{\phi} \varepsilon \delta(t)$ is imposed, where δ is the
 115 Dirac delta function and ε the relative strength of the perturbation, then
 116 correspondingly $q'(t)/\varepsilon \bar{q} = h(t)$, which is why $h(\tau)$ is called the **impulse**
 117 **response** ~~(IR)~~ impulse response. The effects that contribute to flame response
 118 – see Fig. 1 and Eq. (1) – can be investigated separately,

$$h(t) = h_{\Delta H}(t) + h_{s_L}(t) + h_A(t). \quad (5)$$

119 The FTF $F(\omega)$ is obtained from the IR by Laplace transformation, $F(s) =$
 120 $\int_0^\infty e^{-st} h(t) dt$ with $s = -i\omega$.

121 *2.4. Transport of Equivalence Ratio Perturbations*

122 The convective transport of equivalence ratio perturbations ~~is~~ may be
 123 modeled with the ~~1-D-1-D~~ advection equation as

$$\frac{\partial \phi'}{\partial t} + \bar{v} \frac{\partial \phi'}{\partial y} = 0. \quad (6)$$

124 The analytical solution for an impulse perturbation imposed at flame base
 125 $y = 0$ reads

$$\phi'(x, y, t) = \bar{\phi} \varepsilon \delta \left(t - \frac{y}{\bar{v}} \right) = \bar{\phi} \varepsilon \delta \left(t - \frac{X}{\bar{W}} \right). \quad (7)$$

126 Physically interpreted, a sudden change in equivalence ratio at the flame
 127 base convects in y -direction towards the flame tip with the flow velocity \bar{v} .
 128 Eq. (7) also shows how this effect may be represented in the flame-aligned
 129 coordinate system.

130 **3. Contributions to the Flame Impulse Response**

131 *3.1. Fluctuations of Heat of Reaction*

132 The first term on the right hand side of Eq. (1) stands for the contribution
 133 of heat of reaction fluctuations to the heat release rate. The fluctuations
 134 in heat of reaction $\Delta H'$ caused by the equivalence ratio perturbations ϕ'
 135 is approximated by a relation $\Delta H = f(\phi)$ from empirical data (valid for
 136 CH_4 [8]). First order Taylor Series expansion is employed for fluctuating
 137 quantities, $\Delta H' = d\Delta H/d\phi|_{\phi=\bar{\phi}} \phi'$.

138 By integrating $\Delta H'$ over the flame surface, the IR contribution is calcu-
 139 lated as

$$h_{\Delta H}(t) = \frac{1}{\varepsilon} \int_f \frac{\Delta H'}{\Delta \bar{H}} \frac{dA}{\bar{A}} = \frac{1}{\varepsilon} \frac{d\Delta H}{d\phi} \Big|_{\phi=\bar{\phi}} \frac{1}{\Delta \bar{H} \bar{A}} \int_f \phi' dA, \quad (8)$$

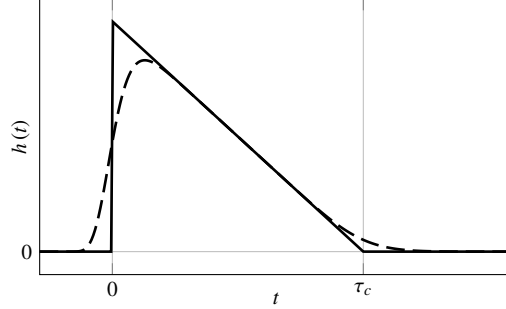


Figure 3: Contribution of fluctuations in heat of reaction or laminar flame speed to the IR. Models without (—) and with dispersion (---)

140 where $\bar{A} = \pi L_f^2 \sin \alpha$ is the steady flame surface area and $dA = 2\pi(L_f -$
 141 $X) \sin \alpha dX$ is the steady infinitesimal flame surface area for a conical flame.
 142 By substituting $\phi' = \bar{\phi} \varepsilon \delta(t - X/\bar{W})$ as defined in Section 2.4, the IR is
 143 obtained in closed form

$$h_{\Delta H}(t) = \frac{2S_{\Delta H}}{\tau_c^2} \{R(t - \tau_c) - R(t) + \tau_c H(t)\}. \quad (9)$$

144 where $H(t)$ is the Heaviside function and $R(t)$ is the Ramp function. $S_{\Delta H} =$
 145 $(\bar{\phi}/\Delta \bar{H}) d\Delta H/d\phi|_{\phi=\bar{\phi}}$ is the sensitivity of the heat of reaction to the equiv-
 146 alence ratio. $\tau_c = L_f/\bar{W}$ is a convective time scale, which is defined as the
 147 time span for the perturbation to travel from the base of the flame to its tip.
 148 The IR is plotted in Fig. 3 with the solid line.

149 ~~By performing~~ Laplace Transform as defined in Section 2.3 ~~, recovers~~
 150 ~~exactly the analytical expression for~~ the flame transfer function ~~defined obtained~~
 151 by Shreekrishna *et al.* [6, Eq. (25)] ~~is recovered.~~

152 For the lean premixed flame, a positive impulse perturbation in the equiv-
 153 alence ratio increases the heat of reaction on the flame surface element located
 154 at the instantaneous position of the perturbation. The increase in heat of
 155 reaction also increases the heat release rate (see Eq. (1)). In Fig. 4 a flame

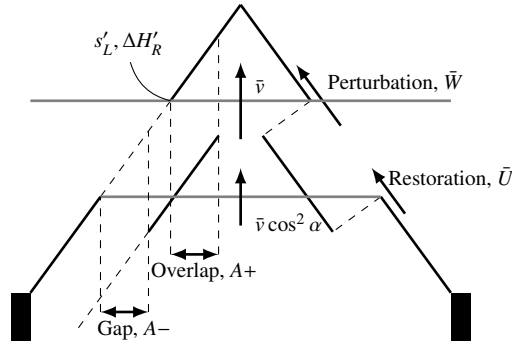


Figure 4: Intermediate flame shape with relevant velocities for convection of perturbation and restoration process. ~~Visualisation~~ Visualization of area gap and overlap due to the change in laminar flame speed

156 perturbed by a δ -pulse as defined in Eq. (7) is shown. The upper gray line
 157 ("Perturbation, \bar{W} ") indicates the flame surface element, whose heat of reac-
 158 tion is changed. The incoming perturbation initially acts on the flame at the
 159 base, which has the largest radius. As the perturbation is convected towards
 160 the flame tip, the resulting perturbation in heat release rate decreases, be-
 161 cause the radius of the flame ~~surface~~ decreases. This fact explains the trend
 162 shown in Fig. 3, that the IR contribution is highest at the beginning and
 163 decreases till the convective time scale τ_c , when the perturbation reaches the
 164 flame tip, which has zero radius.

165 For rich mixtures, additional fuel barely changes the heat of reaction,
 166 which implies that the sensitivity $S_{\Delta H}$ and thus also the corresponding IR
 167 are very small.

168 3.2. Fluctuations of Laminar Flame Speed

169 The second term on the right hand side of Eq. (1) stands for the contri-
 170 bution of laminar flame speed fluctuations to the heat release rate. The same

171 approach as described in Section 3.1 is employed also for laminar flame speed
 172 contribution. The only difference is that $S_{\Delta H}$ is replaced with the sensitivity
 173 of laminar flame speed to the equivalence ratio, $S_{s_L} = (\bar{\phi}/\bar{s}_L) ds_L/d\phi|_{\phi=\bar{\phi}}$.
 174 The shape of the corresponding IR in Fig. 3 can be explained with similar
 175 arguments as Section 3.1. Again, Laplace Transform recovers the FTF of
 176 Shreekrishna *et al.* [6, Eq. (24)].

177 For lean premixed flames the sensitivity S_{s_L} is positive and therefore the
 178 IR is positive. For rich mixtures, additional fuel leads to a decrease in the
 179 laminar flame speed ~~;~~ ~~which indicates that~~ and the IR is reversed.

180 3.3. Fluctuations of Flame Surface Area

181 The third term on the right hand side of Eq. (1) stands for the contri-
 182 bution of flame surface area fluctuations to the IR of the heat release rate.
 183 This mechanism was already discussed by Blumenthal *et al.* [9], albeit only
 184 for the perturbations in velocity. Relevant time scales of restoration τ_r and
 185 convection τ_c were revealed, their impact on flame dynamics was discussed.
 186 In the present study, a similar approach is developed for the effects of equiva-
 187 lence ratio perturbations on flame shape and heat release rate. The similarity
 188 comes from the fact that the perturbed flame position ξ depends on V' and
 189 s'_L , as described in the right hand side of Eq. (3). The similarity is attributed
 190 to Eq. (3), where V' and s'_L act as source terms for the perturbed flame po-
 191 sition ξ .

192 The first step is to compute ξ . The Eq. (3) for $\xi(X, t)$ can be formulated
 193 as an integral equation

$$\xi(X, t) = -\frac{1}{\bar{U}} \int_0^X s'_L \left(X', t - \frac{X - X'}{\bar{U}} \right) dX', \quad (10)$$

194 where laminar flame speed fluctuations caused by ϕ' are considered solely
 195 ($V' = 0$). The IR contribution is calculated as

$$h_A(t) = \frac{1}{\varepsilon} \frac{A'(t)}{\bar{A}} = \frac{2}{\varepsilon L_f^2 \tan \alpha} \int_0^{L_f} \xi(X, t) dX . \quad (11)$$

196 In order to calculate the closed form IR, $\phi' = \bar{\phi} \varepsilon \delta(t - X/\bar{W})$ is substituted
 197 in Eq. (10) and ξ is expressed as

$$\xi(X, t) = - \left. \frac{ds_L}{d\phi} \right|_{\phi=\bar{\phi}} \frac{\bar{\phi} \varepsilon \tau_r}{\tau_r - \tau_c} \left[H \left(t - \frac{X}{\bar{W}} \right) - H \left(t - \frac{X}{\bar{U}} \right) \right] , \quad (12)$$

198 where $\tau_r = L_f/\bar{U}$ is the restorative time scale, which is defined as the time
 199 span for the hypothetical restoration line to travel from the base of the flame
 200 to its tip. ξ is illustrated with an intermediate flame shape perturbed with
 201 an impulse in Fig. 4.

202 The upper gray line ("Perturbation, \bar{W} ") indicates the convection of im-
 203 pulsive perturbation and $\bar{W} = \bar{v}/\cos(\alpha)$ is the projection on X -direction.
 204 Since the mixture is assumed lean and the equivalence ratio perturbation is
 205 positive, the laminar flame speed perturbation is also positive. An increase in
 206 laminar flame speed overcomes the flow velocity normal to the flame surface
 207 and the flame propagates towards the base.

208 Starting from the anchoring point, where $\xi(0, t) = 0$, the restoration
 209 mechanism [9] re-establishes the original, unperturbed flame shape after the
 210 perturbation of equivalence ratio has passed. The lower gray line ("Restora-
 211 tion, \bar{U} ") in Fig. 4 indicates up to which position the restoration process has
 212 progressed. This line travels with the speed $U = \bar{v} \cos(\alpha)$ in X -direction.
 213 The restoration line is upstream of the perturbation line, because of slower
 214 propagation speed.

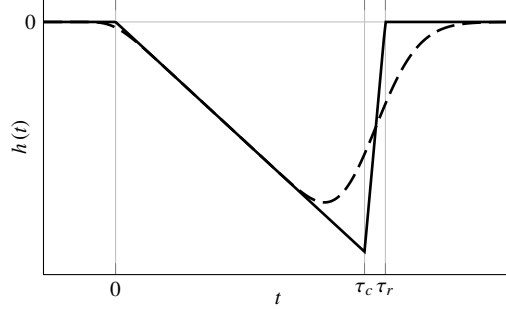


Figure 5: Contribution of fluctuations of flame surface area to IR. Model without (—) and with dispersion (— —)

215 By substituting ξ described in Eq. (12) into Eq. (11), the closed form IR
 216 is obtained

$$h_A(t) = -\frac{2S_{sL}}{\tau_c(\tau_r - \tau_c)} \times \left[\frac{\tau_c}{\tau_r} \{R(t - \tau_r) - R(t)\} - \{R(t - \tau_c) - R(t)\} \right] \quad (13)$$

217 which is plotted in Fig. 5 with the solid line.

218 Again the FTF given by Shreekrishna *et al.* [6, Eq. (26)] is exactly recovered
 219 by Laplace Transform, see Section 2.3.

220 The shape of the IR may be explained as follows: The perturbation ϕ'
 221 causes flame propagation towards the base and creates ~~an~~ additional flame
 222 surface area indicated as "Overlap, A^+ " in Fig. 4. At the same time, the
 223 restoration mechanism brings the flame to its old position and causes a deficit
 224 in flame surface area ~~deficit~~ indicated as "Gap, A^- " in Fig. 4. Since the
 225 restoration process is slower, it acts at a position where the flame radius
 226 is larger than the one for the perturbation, thus the perturbed area is less
 227 than the steady area (negative IR in Fig. 5). As long as both processes
 228 act on the flame together, the deficit of the flame surface area continuously

229 increases. ~~After the perturbation leaves the flame~~At late times $t > \tau_c$, when
230 ~~the perturbation has passed the flame~~, only the restorative mechanism acts
231 to recover the original flame shape. The flame surface area deficit vanishes
232 once the restoration line reaches the flame tip, which corresponds to the
233 restorative time scale τ_r .

234 ~~The FTF of Shreekrishna~~This section concludes with a comment on
235 ~~the study of Cho *et al.* [6, Eq. (26)] is recovered by Laplace Transform, see~~
236 ~~Section 2.3~~[8], who derived time domain representations of flame dynamics
237 by inverse Laplace transformation of frequency domain results. However, the
238 IR was not recovered, because a generic form of perturbations was considered
239 instead of an impulse perturbation. A full time domain analysis of the flame
240 response to a generic perturbation is not straightforward and was indeed not
241 attempted by Cho *et al.* [8]. Instead, their results are valid only in the
242 low-frequency, quasi-steady limit.

243 4. Extended Model with Dispersion

244 In typical technical premixed combustion systems, the fuel is injected
245 from a considerable distance upstream of the flame. This distance is im-
246 portant for the equivalence ratio perturbations because of dispersion due
247 to molecular diffusion for a laminar flame. Generalization to turbulent dis-
248 persion is straightforward, but not discussed further here (refer to Polifke
249 *et al.* [12], Lawn and Polifke [10], Schuermans *et al.* [11] and Bobusch *et*
250 *al.* [13]). As the injection point moves further upstream, a wider Gaussian
251 distribution instead of an impulse (Dirac function) arrives at the flame base
252 and thus the impact on flame dynamics becomes weaker.

253 The model described in Section 2 and also previous models~~[6–8]~~ [\[8, 6, 7\]](#) employ
 254 advection equation as described in Eq. (6). The impact of the species diffu-
 255 sion can be accounted by considering 1-D advection-diffusion equation with
 256 impulse perturbation at flame base $y = 0$, which reads

$$\frac{\partial \phi'}{\partial t} + v \frac{\partial \phi'}{\partial y} = D \frac{\partial^2 \phi'}{\partial y^2}, \quad (14)$$

257 where D is the averaged diffusion coefficient. The analytical solution reads

$$\phi'(x, y, t) = \bar{\phi} \varepsilon \sqrt{\frac{1}{\pi \tau_d t}} \exp \left[-\frac{1}{\tau_d t} \left(t - \frac{X}{W} \right)^2 \right], \quad (15)$$

258 where $\tau_d = 4D/\bar{v}^2$ is the diffusive time scale, which describes the strength of
 259 the diffusion. The solution is expressed in flame aligned coordinate system.

260 The formalism developed in Section 3 can also be applied to the extended
 261 model. For heat of reaction contribution, Eq. (8) is integrated with the dif-
 262 fusive perturbation Eq. (15) instead of the impulse Eq. (7) (same for laminar
 263 flame speed contribution). The resulting IR contribution reads

$$h_{\Delta H}(t) = \frac{S_{\Delta H}}{\tau_c^2} \left\{ \mathfrak{R}(t - \tau_c) - \mathfrak{R}(t) + \tau_c \operatorname{erf} \left(\frac{t}{\sqrt{\tau_d t}} \right) \right\}. \quad (16)$$

264 The contribution of laminar flame speed fluctuations is the same as Eq. (16),
 265 but $S_{\Delta H}$ is replaced with S_{sL} .

266 For flame surface area contribution, the flame surface deviation ξ is de-
 267 termined by integrating Eq. (10) again with the diffusive perturbation. The
 268 contribution is then computed by integrating the flame surface deviation
 269 Eq. (11) as

$$h_A(t) = -\frac{S_{sL}}{\tau_c(\tau_r - \tau_c)} \times \left[\frac{\tau_c}{\tau_r} \{ \mathfrak{R}(t - \tau_r) - \mathfrak{R}(t) \} - \{ \mathfrak{R}(t - \tau_c) - \mathfrak{R}(t) \} \right], \quad (17)$$

270 where $\mathfrak{R}(t, \tau)$ is the smoothed Ramp function defined as

$$\mathfrak{R}(t - \tau) = \sqrt{\frac{\tau_d t}{\pi}} \exp\left(-\frac{(t - \tau)^2}{\tau_d t}\right) + (t - \tau) \operatorname{erf}\left(\frac{t - \tau}{\sqrt{\tau_d t}}\right). \quad (18)$$

271 The resulting IRs are plotted in Figs. 3 and 5 with dashed lines, for heat of
272 reaction (same for laminar flame speed) and flame surface area, respectively.

273 The model can be extended for the cases, where the perturbation is im-
274 posed upstream of the flame base, say $y = -y_0$. The additional time lag for
275 the perturbation to travel till the flame base $\tau_0 = y_0/\bar{v}$ can be accounted by
276 change of variable of $t = t^* - \tau_0$ in Eq. (15)–(17).

277 5. Validation against Numerical Simulation

278 A numerical simulation of a ~~cylindrical burner~~ 2D axisymmetric conical
279 flame is performed to validate the analytical model. ~~The radius is Length and~~
280 radius of the upstream flow duct are both 1 mm long, the mixture is lean, the
281 downstream radius of the computational domain is 6 mm in order to prevent
282 confinement effects. A uniform mesh is constructed with a cell size of 0.02
283 mm. Slip and adiabatic wall boundary conditions are imposed to correspond
284 with the analytical framework. A lean mixture of CH₄ and air ($\bar{\phi} = 0.8$)
285 ~~and the flow is used, the inflow~~ velocity is $\bar{v} = 1$ m/s (Reynolds number
286 130) ~~. Slip and adiabatic walls are assumed for matching the analytical~~
287 ~~framework. at a temperature of 293 K. A 2-step reduced chemistry is em-~~
288 ployed [14] in rhoReactingFoam (OpenFOAM solver), which is modified to
289 assume Prandtl number of 0.7. The averaged molecular diffusivity was set
290 to $D = 0.22 \times 10^{-4}$ m²/s, appropriate for CH₄ in air [15].

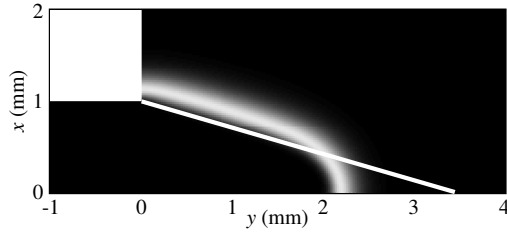


Figure 6: Flame shapes : G-equation model vs. numerical simulation with 2-step chemistry

291 Fig. 6 compares the distribution of steady heat release rate from CFD
 292 against the analytical G -Equation flame. Close to the tip, curvature effects
 293 – which are not considered in G -equation used ~~here~~ results result in a
 294 comparatively shorter flame length of the CFD model.

295 Broadband equivalence ratio perturbations with an amplitude of $\varepsilon =$
 296 $\phi'/\bar{\phi} = 0.05$ are imposed at ~~1 mm upstream of the flame base~~ the inlet. The
 297 corresponding IR is determined via system identification (for details see [16])
 298 and compared against the analytical model in Fig. 7. The latter includes all
 299 three contributions discussed above, see Fig. 1.

300 ~~The averaged molecular diffusivity was set to $D = 0.22 \times 10^{-4} \text{m}^2/\text{s}$, appropriate~~
 301 ~~for CH_4 in air [15].~~ Including dispersion in the analytical model gives a
 302 ”smeared out” response, in qualitative agreement with CFD. More than that,
 303 Fig. 7 shows very good quantitative agreement between CFD and the dis-
 304 persive model for ~~arly period of the impulse response~~ the early period $t < 2$
 305 ms.

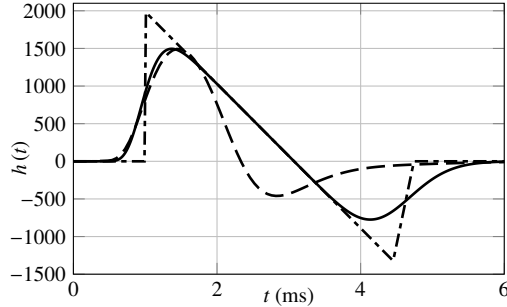


Figure 7: Impulse response functions of conical laminar premixed flame. Analytical model without dispersion (---), with dispersion (—) and CFD results (— · —)

306 At ~~late~~later times, the impulse response is negative before it decays to
 307 zero. This important feature, which is responsible for the excess gain of
 308 the FTF (see below) is reproduced qualitatively by both models based on
 309 the G-equation. Nevertheless, it is apparent that at later times $t > 2$ ms
 310 quantitative agreement with CFD deteriorates. This is due to the over-
 311 predicted flame length of the G-equation model, resulting from the neglect
 312 of curvature effects. Note that the overall duration of the IR is related to the
 313 restorative time scale $\tau_r = L_f/\bar{U}$. Since the flame length L_f is over-predicted,
 314 the resulting IR is also more pronounced at late times.

315 Fig. 8 compares the gain of the FTFs determined with the analytical
 316 model and the CFD simulation, respectively. Important qualitative features
 317 are reproduced by both analytical model formulations: the overall low pass
 318 filter ~~behaviour~~behavior is observed, initial overshoot in gain is present, the
 319 low frequency limit (see Polifke and Lawn [17]) is correctly captured as unity.

320 The dash-dotted line indicates the FTF from the analytical model with-
 321 out dispersion. The model shows oscillatory ~~behaviour~~behavior in the high
 322 frequency range, which is eliminated by dispersion (shown with solid line).

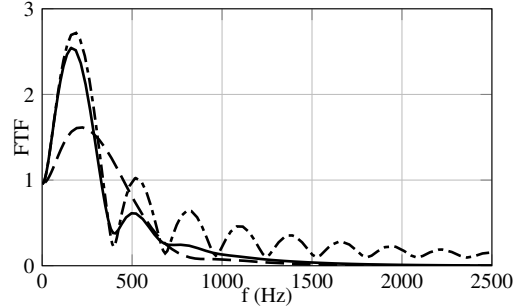


Figure 8: Gain of FTF. Analytical model without dispersion (---), with dispersion (—) and CFD results (— · —)

323 Both analytical and numerical results exhibit excess gain $|FTF| > 1$ at
 324 frequencies around 200 Hz. Excess gain results from constructive superpo-
 325 sition of the positive and negative parts of the IR, as discussed by [Huber](#)
 326 [and Polifke \[18\]](#) and [Blumenthal *et al.* \[9\]](#). The analysis in Section 3 has
 327 shown that the positive part of the IR results from fluctuations in heat of
 328 reaction and flame speed, while the negative part is due to the modulation
 329 of flame surface area. In the low frequency limit ~~the~~ [there is destructive](#) su-
 330 perposition of these effects ~~are destructive, but,~~ [which](#) becomes constructive
 331 at intermediate frequencies, ~~which results resulting~~ in excess gain. Indeed,
 332 earlier models that did not take into account changes in flame surface area
 333 do not exhibit excess gain [12, 19].

334 The intermediate frequency f_{\max} where the gain attains its maximum can
 335 be roughly estimated as

$$f_{\max} \approx \frac{\pi}{2(t_{\max} - t_{\min})}, \quad (19)$$

336 where t_{\max} and t_{\min} are the times where the IR reaches maximal / minimal
 337 values. For the analytical model with dispersion, one estimates $f_{\max} \approx 200$
 338 Hz, which agrees with the gain of the FTF shown in Fig. 8. For the CFD

339 results, the negative part of the IR appears earlier and is less pronounced
340 (see Fig. 6), thus ~~one expects that~~ excess gain occurs at higher frequencies
341 and with reduced magnitude. ~~This is indeed observed~~, as seen in Fig. 8.

342 6. Conclusion

343 The response of laminar premixed flame to equivalence ratio perturba-
344 tions was studied analytically by determining the IR for heat release rate. In
345 the framework of the G -Equation contributions of heat of reaction, laminar
346 flame speed and flame surface area were taken into consideration. Two rele-
347 vant time scales were ~~identifeid~~identified, i.e. a convective time scale τ_c and
348 a restorative time scale τ_r . The transport of equivalence ratio perturbations
349 is related to τ_c , while the propagation of flame shape perturbations along
350 the flame is related to τ_r . The contributions of heat of reaction and laminar
351 flame speed are governed only by τ_c , since the convective perturbations of
352 equivalence ratio causes local changes at the flame surface. The contribution
353 of flame surface area is controlled by both τ_c and τ_r due to the restoration
354 mechanism. Complete agreement with flame transfer functions calculated by
355 Shreekrishna *et al.* [6] was established by Laplace transformation of IRs.

356 An extension to the model was proposed in order to account for the
357 dispersion due to molecular diffusion. The dispersive model adds one more
358 time scale τ_d regarding the strength of the dispersion. As the location of
359 the perturbation moves further away from the flame, its impact on the flame
360 dynamics becomes weaker [12].

361 Analytical models were compared against numerical simulation by exam-
362 ining the respective IRs and FTFs. Quantitative agreement was not achieved,

363 since the analytical ~~*G*-equation~~-Equation model used in this study neglects
364 curvature effects and thus over-predicts the flame length. Nevertheless, very
365 satisfactory qualitative agreement with ~~respee~~-respect to the shape of the
366 IR and the relevant time scales was observed. Overall, the model with dis-
367 persion showed ~~significantly~~-significantly better agreement than the model
368 without dispersion.

369 The analysis in the paper shows that excess gain in the flame response to
370 equivalence ratio fluctuations results from constructive superposition of the
371 effects of fluctuations in heat of reaction and flame speed on the one hand,
372 and the effects of modulation of flame shape on the other.

373 Acknowledgements

374 The presented work is part of the Marie Curie Initial Training Network
375 *Thermo-acoustic and aero-acoustic nonlinearities in green combustors with*
376 *orifice structures* (TANGO). We gratefully acknowledge the financial sup-
377 port from the European Commission under call FP7-PEOPLE-ITN-2012.
378 Financial support for A. Ulhaq was provided by higher education commis-
379 sion (HEC) of Pakistan. Financial support for R. S. Blumenthal was provided
380 by Technische ~~Universität Mu~~Universität München, Institute for Advanced
381 Study, funded by the German Excellence Initiative, and German Research
382 Foundation DFG, project PO 710/12-1.

383 References

384 [1] L. Boyer, J. Quinard, *Combust. Flame* 82 (1990) 51–65.

- 385 [2] A. Fleifil, A. M. Annaswamy, Z. A. Ghoneim, A. F. Ghoniem, *Combust. Flame* 106
386 (1996) 487–510.
- 387 [3] T. Schuller, D. Durox, S. Candel, *Combust. Flame* 134 (2003) 21–34.
- 388 [4] A. R. Kerstein, W. T. Ashurst, F. A. Williams, *Phys. Rev. A* 37 (1988) 2728.
- 389 [5] A. Dowling, S. Hubbard, *Proceedings of the Institution of Mechanical Engineers, Part*
390 *A: Journal of Power and Energy* 214 (2000) 317–332.
- 391 [6] Shreekrishna, S. Hemchandra, T. Lieuwen, *Combust. Theor. Model.* 14 (2010) 681–
392 714.
- 393 [7] S. Hemchandra, in: *ASME Turbo Expo: Turbine Technical Conference and Expositi-*
394 *tion*, GT2011-45590, American Society of Mechanical Engineers, pp. 567–578.
- 395 [8] J. H. Cho, T. Lieuwen, *Combust. Flame* 140 (2005) 116–129.
- 396 [9] R. S. Blumenthal, P. Subramanian, R. Sujith, W. Polifke, *Combust. Flame* 160 (2013)
397 1215–1224.
- 398 [10] C. J. Lawn, W. Polifke, *Combust. Sci. Technol.* 176 (2004) 1359 – 1390.
- 399 [11] B. Schuermans, V. Bellucci, F. Guethe, F. Meili, P. Flohr, O. Paschereit, in: *Int’l*
400 *Gas Turbine and Aeroengine Congress & Exposition*, GT2004-53831.
- 401 [12] W. Polifke, J. Kopitz, A. Serbanovic, in: *7th AIAA/CEAS Aeroacoustics Conference*,
402 *AIAA 2001-2104*, Maastricht, The Netherlands.
- 403 [13] B. C. Bobusch, B. Ćosić, J. P. Moeck, C. Oliver Paschereit, in: *Journal of Engineering*
404 *for Gas Turbines and Power*, volume 136, San Antonio, Texas, USA, pp. 021506–
405 021506.
- 406 [14] J. Bibrzycki, T. Poinso, A. Zajdel, in: *Archivum combustionis*, volume 30, A.
407 *Teodorczyk*, Varsovie, Pologne, 2010, pp. 287–296.
- 408 [15] M. Cowie, H. Watts, *Can. J. Chem.* 49 (1971) 74–77.

- 409 [16] W. Polifke, *Annals of Nuclear Energy* 67C (2014) 109–128.
- 410 [17] W. Polifke, C. J. Lawn, *Combust. Flame* 151 (2007) 437–451.
- 411 [18] A. Huber, W. Polifke, *Int. J. Spray Combust. Dyn.* 1 (2009) 199–228.
- 412 [19] J. F. v Kampen, J. B. W. Kok, T. H. van der Meer, in: 12th Int. Congress on Sound
413 and Vibration (ICSV12), IIAV, Lisbon, Portugal, July 11-14 2005.

Preprint

Rebuttal for Manuscript PROCI-D-15-00274

“An Analytical Model for the Impulse Response of Laminar Premixed Flames to Equivalence Ratio Perturbations”

by Albayrak et al.

Reviewer #1: Very Good

Does the English in this paper need to be improved? 3 (NO)

This paper describes an analysis of the impulse response of a premixed flame to fuel/air ratio disturbances. This is the first study that I am aware of that has executed this analysis and I recommend it for publication. A few suggestions for the authors:

1) Some of the general overview sections (e.g., Sec. 2.2) can be reduced to allow the authors more space to discuss results; authors can refer to entire chapter on related problems in text "Unsteady Combustor Physics" or comparable reference.

The paper gives essential background information in order to make the presentation self-contained (while respecting the page limit). We want to keep it that way; therefore the overview section has not been shortened significantly. As suggested, a reference to "Unsteady Combustor Physics" has been added.

2) One of the first studies to look at FTF's of this fuel/air ratio forced problem was Ann Dowling - it would be appropriate to acknowledge that work in the intro; e.g. A.P. Dowling, S. Hubbard, Proc. Inst. Mech. Engrs. 214 (A) (2000) 317-332.

Thanks for pointing this out! The work of Dowling and Hubbard is now mentioned in the introduction (page 3 lines 18-20).

3) Ref. 7 also includes time domain expressions for the flame response to arbitrary time varying fuel/air ratio disturbances in Appendices A and B. Would be worth discussing the impulse response characteristics in the context of those results.

The link between Impulse Response (IR) and FTF can be established in both time and frequency domain. The frequency domain formulation is well established in combustion dynamics, also the core text in Ref [7] is formulated in the frequency domain. Arriving at a time domain representation by applying an inverse Fourier Transform is a purely mathematical operation, which does not easily allow physical interpretation. Establishing the correspondence in frequency domain will be more convincing and more informative for the majority of readers, and that is why we have chosen this option. Furthermore, one should note that the IR is not recovered in [7], since a generic

perturbation is used instead of an impulsive perturbation. The full analysis based on such a generic perturbation is not straightforward and not even attempted in [7]. Instead, the time domain approach is used to investigate merely the low frequency limit of the flame response. This limit may be recovered as from our results. Contrary to that, our work gives a complete (!) time domain analysis, and thus allows a better understanding of how perturbations interact with the flame. These points are emphasized in the revised manuscript (page 14, lines 213-220).

4) This same reference notes that the flame response to fuel/air ratio disturbances cannot be cast in the form of only an n-tau model (unlike the response of the flame to velocity disturbances) in the $St \ll 1$ limit - there is an additional derivative term. Again, suggest using these results to interpret that result.

Unfortunately, I cannot reproduce this statement. Assuming $St \ll 1$, my calculation leads

$$Q' = S_H \left\{ \delta(t) - \frac{\tau_c}{3} \delta'(t) \right\} + S_s \frac{\tau_r}{3} \delta'(t)$$

But in Ref.[7];

$$Q' = S_H \delta \left(t - \frac{\tau_c}{3} \right) + S_s \frac{\tau_r}{3} \delta'(t)$$

Therefore, we do not follow the reviewer's suggestion.

Preprint

Reviewer #2: Marginal

Does the English in this paper need to be improved? - 3 (NO)

The response of a conical flame subjected to fluctuations of equivalence ratio is studied using a methodology based on an impulse function, introduced by Blumenthal et al. [8]. The mathematical model is based on a linearized G-equation with a prescribed incoming flow, i.e., unaffected by the heat of release, further simplified by assuming the nature of the fluctuations in flame speed and flame surface area, and assuming that the heat of reaction is a specified function of equivalence ratio. Given all these ad-hoc assumptions I am not surprised that the results are made to agree with the transfer functions calculations of Ref. [5]. Since the model is based on phenomenology and not on fundamental physical principles, it is difficult to judge its importance and value. In my opinion, this work is a nice pedagogical exercise but does not contribute much our understanding of flame instability.

The second reviewer graded the manuscript as „Marginal”, yet did not contribute any specific recommendations on how to improve the paper. This is inappropriate and we argue that the validity, originality and novelty of our work were not appreciated by the reviewer in an adequate manner:

- By the statement "assuming the nature of the fluctuations in flame speed and flame surface area", the reviewer criticizes the time-domain approach as an ad-hoc model „made to agree with ... Ref. [5]”. However, there exists solid theory that flame surface modulations are caused by kinematic balance between flow and flame speed, which can be represented as a level set approach using the G-equation. Obviously, the approach is not ad-hoc and indeed this type of model is widely used by others [2,3,5,7,8]. We thus dismiss the reviewer’s statement as unqualified. Similarly, the relations for steady state laminar flame speed and heat of reaction as a function of equivalence ratio are based on theory or experimental evidence (and used by other authors, e.g. Ref. [7]). Starting from the same premises, we find that the time domain approach does reproduce the results of frequency domain analysis and is thus validated - but this does not mean that our results were „made to agree”! We emphasize that there was no “tuning of parameters” whatsoever.*
- Reviewer #2 also comments that „this work is a nice pedagogical exercise but does not contribute much to our understanding of the flame instability”. This statement reads like a contradiction in terms! The work is to indeed to some extent pedagogic in nature, as it brings insight and understanding to the problem of transient flame dynamics - including relevant time scales - that cannot be developed easily from a frequency domain analysis.*
- The reviewer does not appreciate that our time domain solution is extended by including the dispersion of equivalence ratio perturbations. This is an important novelty, compared to previous studies [5-7]. Again one sees that the reviewer's opinion (“ does not contribute much our understanding of flame instability.”) is not justified*

Reviewer #3: Very Good

Does the English in this paper need to be improved? 3 (NO)

This article proposes an analysis of the dynamic response of laminar conical flames to equivalence ratio perturbations. The analysis is carried out in the time domain. The fluctuations of heat release are represented in terms of a sum of impulse responses corresponding to the various response functions involved.

The model results are compared with numerical simulations of a laminar flame.

This is a well written article and it touches a problem of interest. The mathematical developments seem to be right and they have been checked by taking the Laplace transform of the impulse response functions and comparing with results published previously. This is however not shown and it would be worth providing expressions for this Laplace or Fourier transforms which could be compared with those existing in the literature.

We excluded the Laplace transformed expressions due to the page limit. Instead, we are emphasizing that the Laplace transformed results are exactly same with the FTF expressions defined by Shreekrishna et al. [6] and we address the specific equations in that paper. (see page 9 lines 129-131, page 11 lines 157-159 and page 13 lines 197-199)

For the CFD it would be of interest to give some details on the computational mesh. One is always attentive to the number of grid points used to resolve the flame. It would also be worth indicating that the calculations were carried out in an axisymmetric framework (if this is indeed the case).

Additional information related to the numerical approach is provided in Section 5 (page 16-17, line 255 – 275).

Concerning the originality of the contents of this manuscript, the authors should state more clearly what is new with respect to the earlier work of Cho and Lieuwen (Ref. [7]). This last reference contains in its appendix B a time domain analysis of the impulse response of a conical flame submitted to equivalence ratio perturbations. One may wish to know if results like expression (13) coincide with those given in the appendix of Ref. [7]. There is a familiar look but I did not try to check this in detail...

The extended model with dispersion seems to be new but what about the material in section 3?

Please see our response to the 3rd point of Reviewer #1. Same arguments as discussed there apply also here. This is discussed in the revised manuscript (page 14, lines 213-220).

It would be interesting to point out that the CFD and the analytical results do not agree well at all. At present the cause of this important difference is not discussed in the core of the text. In the conclusion, the difference is attributed to the curvature effect which is not included in the G-

equation. If the calculations had been carried out on a flame established by a larger diameter injector, the curvature effect would have been of lesser importance but it is probable that the difference would still be there.

The discussion related to the curvature effect has been added to the revised manuscript (see page 18 lines 280-288). It is true that that the curvature is less important for longer flames, and agreement between CFD and the analytical results should increase. However, without further investigation it is not appropriate to speculate about this in this paper.

While the previous points are important, this article is nevertheless interesting and deserves to be presented after revision.

Other comments

Correct typos like those appearing in page 18 « arly » ? or in page 19 where « identifid » should be replaced by « identified » or in page 21 where « respec » should be « respect »...

Typos are corrected in the revised manuscript.

Flow conditions corresponding to figure 6 need to be specified.

Boundary conditions for inlet flow velocity and equivalence ratio were already defined. In the revised manuscript, the inlet temperature is also included (see pages 16-17 lines 262-263). The results are now reproducible with the given information.